

Dedicated to Prof. Edith A. Turi in recognition of her leadership in education

TMDSC AND DYNAMIC RHEOMETRY GELATION, VITRIFICATION AND AUTOACCELERATION IN THE CURE OF AN UNSATURATED POLYESTER RESIN

G. Van Assche¹, E. Verdonck² and B. Van Mele^{1}*

¹Vrije Universiteit Brussel, Dept. for Physical Chemistry and Polymer Science, Pleinlaan 2
1050 Brussel

²TA Instruments Benelux, Waters, Raketstraat 60, 1130 Brussel, Belgium

Abstract

The free radical cross-linking copolymerization of an unsaturated polyester resin with styrene is studied in isothermal conditions using temperature modulated differential scanning calorimetry (TMDSC) and dynamic rheometry. The dynamic rheometry measurements show that gelation occurs at a conversion below 5%, while TMDSC measurements show that an important autoacceleration starts near 60% conversion, giving rise to a maximum cure rate closely before the (partial) vitrification of the system near 80%. This indicates that the autoacceleration is not due to the sharp increase in bulk viscosity at gelation, but rather to a change in molecular mobilities at higher conversion.

Keywords: autoacceleration, dynamic rheometry, gelation, gel effect, TMDSC, unsaturated polyester resin, vitrification

Introduction

A characteristic phenomenon for the free radical polymerization of certain monomers is that at intermediate-to-high conversions a dramatic increase in the rate of polymerization occurs, often accompanied by a marked rise in temperature [1]. The term ‘gel effect’ was coined for this phenomenon due to the characteristic rise in viscosity accompanying the rapid increase in monomer conversion [2]. Although this phenomenon was first noted more than 50 years ago [3, 4], and although the gel effect is well understood in general terms of a decrease in mobility of growing chains, its detailed mechanism is still a matter of discussion [1].

According to Norrish and Smith [4], the most likely explanation for the gel effect is a decrease in the rate parameter for chain termination, leading to an increased radical concentration. They postulated that the increased viscosity, caused by an increased conversion of monomer to polymer, can be correlated with a decrease in the mobility of the growing chains, making it more difficult for them to diffuse together and terminate.

* Author to whom all correspondence should be addressed.

Trommsdorff *et al.* [5] showed that the gel effect occurs earlier when pre-dissolved polymer is included in the initial reaction mixture. On the other hand, the gel effect onset tends to be delayed for polymerizations performed in the presence of solvent [2, 6]. Both observations corroborate the conclusion that the gel effect is caused by an increase in bulk viscosity. This early work indicates the importance of a diffusion-controlled termination step: the bulk viscosity would not affect the termination rate parameter if this reaction step was chemically-controlled.

The idea that the increasing bulk viscosity causes the gel effect has gradually evolved over the years. Important concepts introduced include the notion of local resistance-to-motion or 'microviscosity' (rather than bulk viscosity) [1], and the short-long termination concept [7–10].

It should be stressed that 'gelation' and 'gel effect' are different phenomena. At *gelation*, the material changes from the initial viscous state to a rubbery or energy-elastic state because covalent bonds connect across the whole volume of the curing material [11, 12]. The structure formed at the *gel point* is termed the *critical gel*. According to Winter [13, 14], the *gel point* of a chemically cross-linking system is defined unambiguously by the instant at which the mass average molecular mass diverges to infinity. Consequently, the steady flow viscosity diverges to infinity and an equilibrium shear modulus develops, at first for frequencies tending to zero [15].

Although gelation and the gel effect might be correlated for cross-linking free radical polymerizations, both phenomena can occur independently. Indeed, the formation of a chemical gel is related to network formation and occurs in both step-growth and free radical chain-growth *cross-linking* systems, but per definition not in *linear* polymerizations. In contrast, the gel effect is limited to free radical polymerizations and occurs in both *linear* and *cross-linking* polymerizations. As a matter of fact, it was first observed and mostly studied for linear systems.

As summarized by te Nijenhuis [15], several methods are used for the determination of the gel point. Discussions about specific aspects of equilibrium and dynamic rheometry measurements can be found in [11–15]. Early rheological studies of unsaturated polyester cure include [17, 18]. Later rheological data were combined with kinetic studies using DSC [19–24].

Hsu and Lee [25, 26] used a solvent extraction procedure to determine the gel fraction during the first stages of the unsaturated polyester-styrene copolymerization. Their results point out that the gel point occurs before the crossover of G' and G'' , at overall monomer conversions lower than 2%. In general, gelation is observed at the very beginning of the curing reaction, at a conversion lower than 5% [24–28]. After the gel point, a continued increase in G' and a maximum in G'' can be ascribed to vitrification [17, 24, 29], which is the transition from a rubbery or liquid state to a glassy state due to the increasing glass transition temperature [30]. The maximum in G'' shifts forward when the frequency is increased [29].

For the free radical copolymerization of unsaturated polyester or vinyl ester resins with styrene, the gel effect is seldom mentioned or observed. For the modeling of the reaction kinetics the termination reaction is often neglected: the system is treated as if the gel effect is present from the start and there is never a balance between

initiation and termination steps [28, 31–33]. If termination involving small radicals is negligible, the termination reaction might be insignificant after gelation [31].

One of the main problems for accurate measurements of the gel effect is the difficulty of maintaining isothermal conditions in bulky samples. In a recent review, O'Neil and Torkelson [1] point out isothermal DSC measurements might be advantageous to achieve truly isothermal conditions. In this paper it will be shown that the use of temperature modulated differential scanning calorimetry (TMDSC) in isothermal reaction conditions brings additional advantages over using the conventional DSC technique, especially for indicating the location of the gel effect with respect to the vitrification of the polymerizing system. In previous publications [34–38] it was shown that TMDSC is very suited for studying vitrification, because the chemical reaction and the vitrification phenomenon can be followed simultaneously using the heat flow and heat capacity signals, respectively. First results on unsaturated polyester and vinyl ester resins were mentioned in [37].

Materials and techniques

Materials

An unsaturated polyester resin containing 45% by mass of styrene (Polylite 51383, Reichhold) was cured with a peroxide initiator (Butanox M60, AKZO) and a cobalt octoate accelerator (NL49S, AKZO) in a ratio of 100:2:1 by mass. A weight fraction of 200 ppm inhibitor (2-methylhydrochinon) was added for delaying the reaction during sample handling.

The polyester prepolymer of the PolyLite 51383 resin is made of fumaric acid, maleic acid, tetrahydrophthalic acid, neopentylene glycol and diethylene glycol. Its number average molecular mass equals 1850 g mol^{-1} (by GPC). The molar ratio of styrene vs. polyester vinylene bonds equals 4.1:1 (by $^1\text{H-NMR}$ and $^{13}\text{C-NMR}$). The average number of vinylene bonds per polyester prepolymer is 3.5. A small amount of inhibitor is present in the resin. The glass transition of the fully cured material is $30^\circ\text{C} \pm 5^\circ\text{C}$ and the transition is ca 50°C wide.

Techniques

TMDSC

TMDSC measurements were performed in hermetic pans on a *TA Instruments* DSC 2920 with MDSC[®] option, using a 0.5°C amplitude and a 60 s period. After (quasi-)isothermal curing, the glass transition temperature of the isothermally cured material and the residual heat of reaction were determined by cooling the sample to -60°C and heating to 225°C at 5°C min^{-1} . In a second cool-heat cycle the final glass transition temperature was determined. The conversion and rate of conversion are calculated as

$$x = \frac{\Delta H_p}{\Delta H_{\text{tot}}} \quad \text{and} \quad \frac{dx}{dt} = \frac{dq/dt}{\Delta H_{\text{tot}}} \quad (1)$$

with ΔH_p and ΔH_{tot} the partial and total reaction enthalpies, and dq/dt the measured non-reversing heat flow. The total reaction enthalpy ΔH_{tot} equals 320 J g^{-1} .

The variation in the heat flow phase angle was always limited to a few degrees. Thus, the modulus of the complex heat capacity and the in-phase component will (nearly) coincide [36–38]. In this paper, the term heat capacity will be used, without further specification.

Dynamic rheometry

Dynamic rheometry measurements were made with a *TA Instruments* AR1000-N rheometer in parallel plates mode using disposable aluminum plates with a 4 cm diameter, at an oscillation frequency of 1 Hz. A calibrated reference oil for viscosity (Poulsen, Selfe & Lee Ltd, 924.5 mPa s at 20°C) was used to check the calibration.

For the instrument setup employed, it is important to note that when the shear modulus increases above approximately $5 \cdot 10^5$ Pa the results are not quantitative anymore due to an important contribution of the instrument's compliance. In order to avoid overloading of the normal force load cell due to polymerization shrinkage, the gap was reduced using *TA Instruments* Navigator software.

To study the influence of frequency, measurements were performed at frequencies of 0.1 and 1/60 Hz. Due to relatively long equilibration times at the lower frequencies, few points can be measured before gelation.

Dynamic mechanical analysis

To quantify the properties of the fully cured material, dynamic mechanical analyses were performed on a *TA Instruments* DMA 2980 in single cantilever mode using samples of ca. $40 \times 7 \times 1 \text{ mm}^3$. Isothermal measurements at selected temperatures for frequencies of 1, 0.1, and 1/60 Hz, and non-isothermal experiments at 1°C min^{-1} at a frequency of 1 Hz were performed.

Results and discussion

TMDSC study of the isothermal cure of unsaturated polyester

Autoacceleration

The evolution of the non-reversing heat flow for the curing of the unsaturated polyester resin at 30, 40 and 50°C is shown in Fig. 1. Some numerical data are summarized in Table 1.

The heat flow evolution can be divided into three stages. At 30 and 40°C an *inhibition period* is observed.

Once the inhibitor is consumed, the free radical concentration quickly increases and the polymerization accelerates, leading to the *main reaction exotherm* with a maximum close to 12% conversion. The intensity of the maximum increases by more than a factor 2.5 by increasing the temperature from 30 to 50°C.

Table 1 TMDSC results for the cure of an unsaturated polyester system at different isothermal cure temperatures (T_{cure}). Time, conversion x , and non-reversing heat flow dq/dt at the first maximum, the minimum, and the second maximum in the non-reversing heat flow. t_{onset} is the time at the onset of the main reaction exotherm

$T_{\text{cure}}/$ °C	$t_{\text{onset}}/$ min	First maximum			Minimum			Second maximum		
		t/min	x	dq/dt mW g^{-1}	t/min	x	dq/dt mW g^{-1}	t/min	x	dq/dt mW g^{-1}
30	37	65	0.14	25	177	0.58	19	219	0.73	20
40	15	29	0.11	42	95	0.57	30	121	0.72	34
50	–	15	0.10	66	62	0.58	43	80	0.74	49

Near a conversion of 58% a minimum is reached, which is followed by an *auto-acceleration* towards a second heat flow maximum. At first sight, this auto-acceleration might seem to be rather limited since the heat flow (and thus the reaction rate) at the second maximum is only 10 to 14% above the minimum. However, one should bear in mind that the concentration of reactive units is continuously decreasing: in-between the autoacceleration onset and maximum the concentration of reactive units decreases by more than a factor 1.5. This monomer depletion has an important decreasing tendency on the rate of reaction, which is more than compensated by the autoacceleration effect. To take the monomer depletion into account, the reduced rate of conversion R_r is calculated.

The reduced rate of conversion R_r is calculated by dividing the rate of monomer consumption by the monomer concentration:

$$R_r = Y - \frac{1}{[M]} \frac{d[M]}{dt} = \frac{dx/dt}{(1-x)} = k_p [R^*] \quad (2)$$

with $[M]$ and $[R^*]$ the concentrations of monomer and propagating radicals, respectively, and with x the conversion of monomer. Thus, the reduced rate of reaction reflects changes in the concentration of propagating radicals and in the (apparent) propagation rate constant k_p .

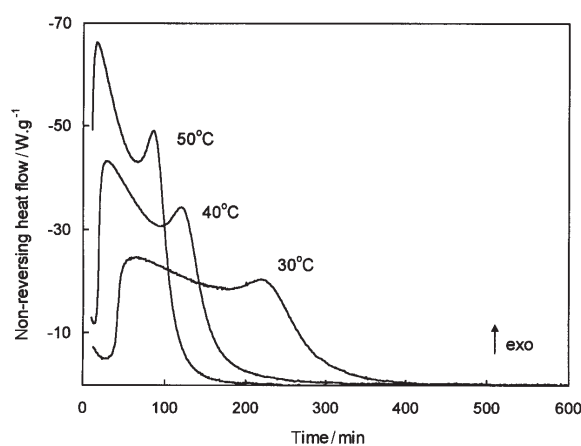


Fig. 1 Non-reversing heat flow for the isothermal cure of an unsaturated polyester at 30, 40 and 50°C

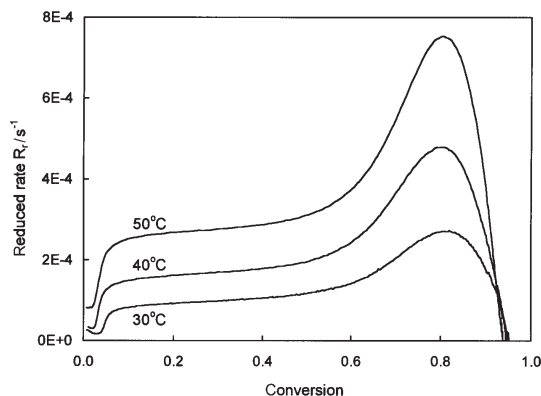


Fig. 2 Reduced rate of reaction vs. conversion for the isothermal cure of an unsaturated polyester at 30, 40 and 50°C

For the experiments of Fig. 1, the evolution of the reduced rate of conversion as a function of conversion is given in Fig. 2. After the inhibition period, in which a few percent of conversion occurs, R_r sharply increases to a level which is higher with increasing temperature. This sharp rise is due to the strong increase in the concentration of propagating radicals when the inhibitor has been consumed. Once the plateau is reached, R_r increases slowly up to 50% conversion. Subsequently the autoacceleration effect is observed as an almost threefold increase in R_r caused by a further increase in the concentration of propagating radicals due to diffusion limitations in the termination step. The maximum value of R_r is attained near 80% conversion. Diffusion limitations on the rate of propagation will tend to decrease the (apparent) propagation rate constant, thus reducing R_r . The ultimate conversion attained isothermally is less than unity (ca 95%), which points to the occurrence of vitrification during the isothermal cure experiments.

Vitrification

The occurrence of vitrification is confirmed by a downward step in the heat capacity C_p which starts close to the autoacceleration maximum in the non-reversing heat flow (indicated with a small circle) (Fig. 3). Afterwards C_p evolves to a constant level. This stepwise decrease in heat capacity is characteristic for vitrification [34, 35]. The glass transition of the fully cured resin is shown in Fig. 4. It is observed as an increase in C_p and as a downward peak in the heat flow phase ϕ . The transition midpoint is close to 30°C, but the transition stretches at least from 10 to 60°C. At these temperatures the fraction of material that is in the vitrified (glassy state) equals 90 and 10%, respectively. This fraction, also termed *degree of vitrification*, was calculated using reference lines for the glassy and the rubbery state (Fig. 4) and corresponds to $1-DF^*$ (with DF^* the mobility factor as defined in [34, 35]). The cure temperatures studied (30, 40, and 50°C) are clearly within the broad glass transition interval of the fully cured material. Thus, at these temperatures the fully-cured material is in a partially

glassy – partially rubbery state (for the modulation frequency used). At a higher temperature less material is vitrified. Hence, the height of the step-wise decrease in C_p decreases strongly with increasing cure temperature (Fig. 3). The final degree of vitrification equals 50, 30 and 20%, for 30, 40 and 50°C, respectively. The term *partial vitrification* was coined for this vitrification phenomenon in which the final state reached isothermally is only partially glassy [37]. This occurs when a thermoset is cured at temperatures within the glass transition region of the fully-cured resin. This partial vitrification should not be confounded with a partially vitrified intermediary state that occurs while the reaction is still continuing.

The partial vitrification can also be noted in the heat flow phase evolution. In Fig. 3, ϕ starts decreasing at the onset of vitrification and then evolves to a constant

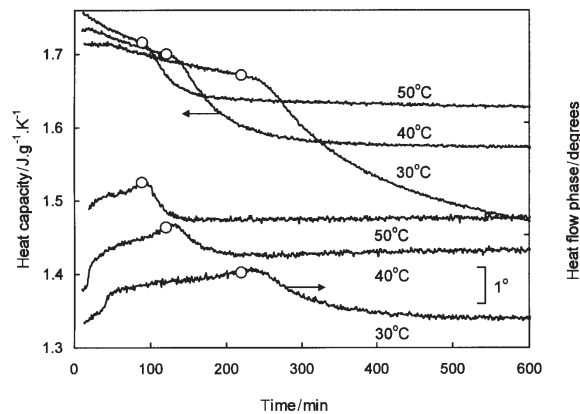


Fig. 3 Heat capacity and heat flow phase for the isothermal cure of an unsaturated polyester at 30, 40 and 50°C. The heat flow phase curves were shifted vertically to avoid overlap. The symbols (o) denote the points at maximum cure rate in the non-reversing heat flow

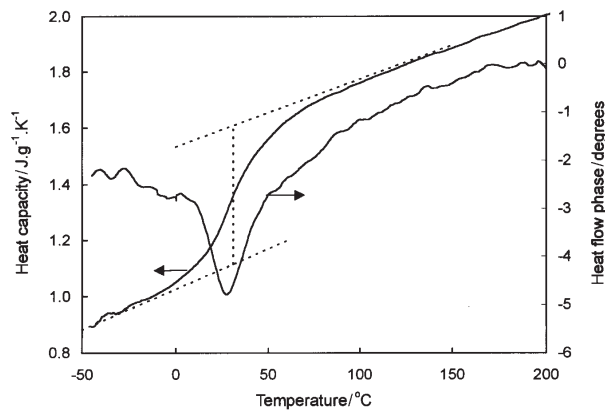


Fig. 4 Heat capacity and heat flow phase for the glass transition of a fully cured unsaturated polyester (TMDSC at 5°C min⁻¹)

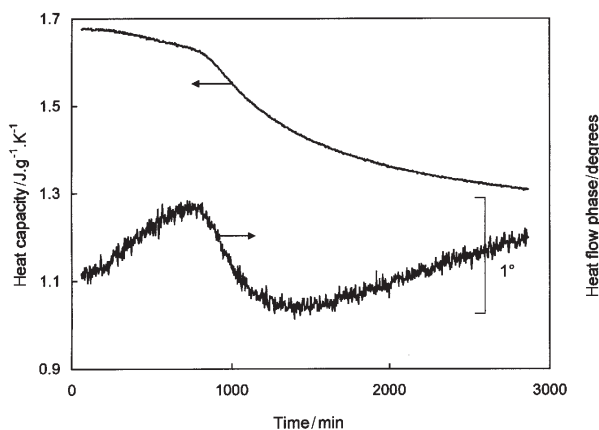


Fig. 5 Heat capacity and heat flow phase for the isothermal cure of an unsaturated polyester at 0°C. No extra inhibitor added to formulation

level. The heat flow phase remains at a low (more negative) value because the cure temperatures are above the temperature of maximum relaxation of the fully cured network (Fig. 4). If the resin is cured at lower temperatures, e.g. at 0°C, the heat flow phase passes through a minimum and increase again to its final, more glassy level (Fig. 5). At 0°C, the rate of reaction is too slow for a quantitative analysis of the heat flow. The evolution of heat capacity and heat flow phase, however, can still be measured accurately, illustrating an extra benefit of TMDSC to study isothermally slow reacting systems (notice the extended time scale of Fig. 5).

Partial vitrification has already been discussed for epoxy resins [37], but the temperature interval in which partial vitrification can be observed is much narrower (Fig. 12 in [37]). More recently, Montserrat and Cima [39] presented similar epoxy cure experiments, but their interpretation is somewhat misleading. The way the mobility factor DF^* was calculated is in contradiction with the fact that the final state is only partially glassy for cure temperatures that are within the glass transition of the fully-cured resin, as was explained in detail in this paper. Only with the correct definition of the reference states (same temperature and conversion [35]) the points for which DF^* equals 0.5 will correspond to the *vitrification point* for which T_g equals the cure temperature.

Finally, attention is drawn to the slow decrease in C_p before the onset of vitrification (Fig. 3). This decrease is linear with reaction conversion, with a slope equal to $-0.058 \pm 0.005 \text{ J (g K)}^{-1}$ per unit of conversion**. This decrease can be attributed to the chemical changes upon curing: the heat capacity of the polymer (in the liquid and rubbery state) is lower than the heat capacity of the uncured, liquid resin. For epoxy resins more complex changes in heat capacity before vitrification were attributed to reactions with primary and secondary amine [37].

** Average and standard deviation for experiments at 30, 40 and 50°C. Slope calculated from 0 up to 75% conversion (just before vitrification sets in).

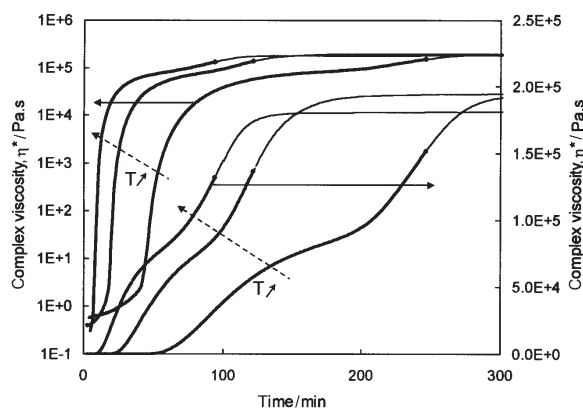


Fig. 6 Complex viscosity for the isothermal cure of an unsaturated polyester at 30, 40 and 50°C. η^* is plotted both on a linear and a logarithmic scale. Above a certain viscosity level the curves are not quantitative anymore (thinner lines, see text)

Rheological changes upon isothermal cure of unsaturated polyester

Evolution of the complex viscosity

Because the autoacceleration or gel effect is generally attributed to the strong increase in viscosity upon polymerization, the rheological changes during cure were studied using isothermal small amplitude oscillatory shear measurements or dynamic rheometry. For cure experiments at 30, 40 and 50°C, the evolution of the complex viscosity η^* is given in Fig. 6, both on a linear and a logarithmic scale. A comparison of the evolution of $(\log) \eta^*$ and the non-reversing heat flow at 40°C is shown in Fig. 7 (for TMDSC at other temperatures, Fig. 1). A first and strong increase in η^* occurs before the first maximum in the heat flow, for less than 10% conversion. Close to the onset of autoacceleration (ca 60% conversion) and slightly before the onset of vitrification, a second increase in η^* is observed (Figs 6 and 7). The level attained at the end of this second increase is underesti-

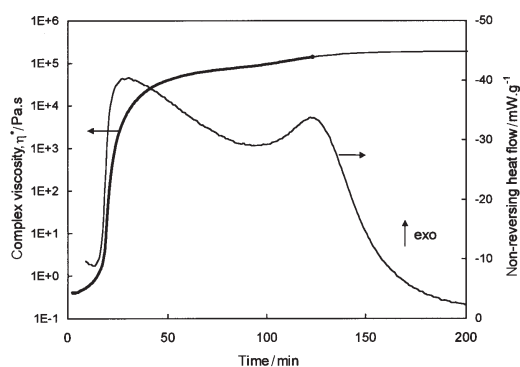


Fig. 7 Comparison of complex viscosity and non-reversing heat flow for the isothermal cure of an unsaturated polyester at 40°C. η^* is plotted on a logarithmic scale

mated due to the contribution of the instrument's compliance to the displacement measured.

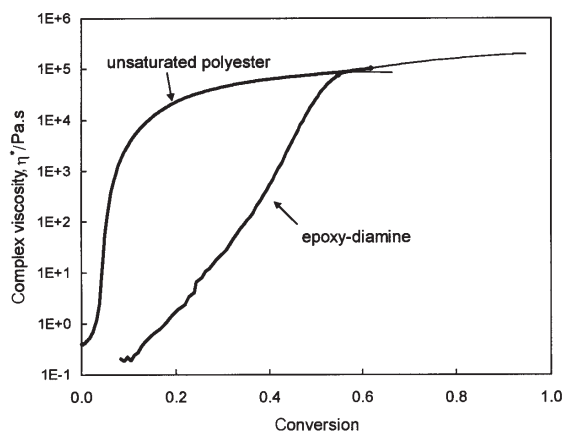


Fig. 8 Comparison of complex viscosity with conversion for the isothermal cure of an epoxy – diamine system at 60°C (results from [40]) and the isothermal cure of an unsaturated polyester at 40°C. Viscosity plotted on a logarithmic scale

Before discussing the phenomena, it is interesting to point out that the observed evolution is quite different from the evolution for step-growth polymerization thermosetting systems. In a step-growth (bifunctional) epoxy-(tetrafunctional) amine system, the viscosity rises continuously with extent of polymerization (Fig. 8); gelation occurs near 60% conversion [40]. The different conversion-dependence of η^* is related to the molecular mass evolution and network development: for addition step-growth polymerization systems the molecular mass of the polymer chains gradually increases, while for (linear) free radical chain-growth polymerizations the highest average degree of polymerization of the polymer chains is attained at the start of the reaction.

Gelation and gel point determination

The evolution of the storage and loss shear moduli, G' and G'' , and the mechanical loss angle δ , gives additional information concerning the rheological changes (Fig. 9). With increasing temperature, the transitions move forward, but the curve shape changes little. Initially, the material behaves like a viscous liquid (δ close to 90°), with a complex viscosity in the order of 10^{-1} Pa s. During the inhibition period (Fig. 1), G'' increases slightly, while G' , first too small to be measured accurately, increases much faster. Then *gelation* occurs: within a 5 min time span δ drops from more than 85° to less than 5°, implying a fast change of the rheological behavior from viscous-like to rubbery-like (entropy-elastic behavior). At the same time, G' , G'' , and η^* increase more than a factor 10^3 , 10 , 10^2 , respectively, and crossover between G' and G'' occurs ($\delta=45^\circ$). The detailed data in Table 2 show that the complex viscosity is less than 10 Pa s at the crossover point. This value is unexpectedly low for the crossover point to correspond to the gel point, since the zero

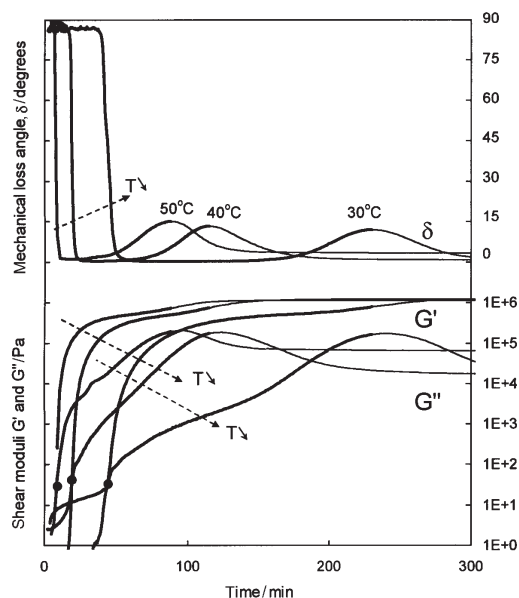


Fig. 9 Storage and loss shear moduli and mechanical loss angle for the isothermal cure of an unsaturated polyester at 30, 40 and 50°C at 1 Hz. Moduli plotted on a logarithmic scale

shear rate viscosity should tend to infinity at the gel point [11–15]. However, if the extrapolated evolution of the reciprocal complex viscosity is considered, the gel times obtained correspond quite well with the time at the crossover point.

These results point in the direction of gelation at an extent of reaction below 5%, which is in agreement with literature [24–28, 41].

Vitrification and final cure stages

As the cure continues, δ increases again, and while δ and G'' attain a maximum, a stepwise increase is observed for G' and η^* . Both the stepwise increase in G' , the maximum in G'' , and a final mechanical loss angle close to zero are indications that *vitrification* takes place [17, 24, 29], in agreement with the TMDSC data.

The final storage modulus obtained by dynamic rheometry is too low for a glassy solid: due to the high moduli, the instruments' compliance dominates the response, and the final evolution is not quantitatively measured. A non-isothermal DMA experiment for fully cured samples resulted in storage moduli of 2.0 GPa (30°C), 1.2 GPa (40°C), and 0.32 GPa (50°C). For the rubber plateau, a value of 3.9 MPa is obtained at 90°C. Thus, for the isothermal transition from the rubbery to the glassy state an increase in modulus of at least three orders of magnitude would be expected (30°C is at the lower limit of the transition zone), much larger than the increase observed by dynamic rheometry.

Table 2 Dynamic rheometry results for the cure of an unsaturated polyester system at different isothermal cure temperatures (T_{cure}) and frequencies. Time, complex viscosity η^* , storage shear modulus G' , and TMDSC conversion at the crossover point of storage and loss shear moduli G' and G'' . Time to onset of the final increase in storage shear modulus G' and to onset of the final decrease in heat capacity (C_p) measured in TMDSC

$T_{\text{cure}}/$ °C	Crossover G' and G'' at 1 Hz				Time onset vitrification in min			
	Time/ min	$\eta^*/$ Pa s	$G'/$ Pa	x	$G'/$ 1 Hz	$G'/$ 0.1 Hz	$G'/$ 1/60 Hz	$C_p/$ 1/60 Hz
30	44	7	33	3%	212			248
40	19	9	42	4%	108			131
50	9	7	29	2%	81	98	104	95

Although the final stages can not be quantitatively measured by dynamic rheometry, the onset of the final increase in G' (and δ) can be used as a measure of the onset of vitrification. Comparison of the numerical TMDSC and the rheometry results (Table 2) shows that the onset of vitrification in TMDSC (at 1/60 Hz) occurs later than the onset of the increases in the moduli (at 1 Hz). One reason for this difference is the frequency dependence of the glass transition and, by consequence, vitrification. Therefore, the effect of frequency on the dynamic rheometry measurements was investigated (Fig. 10).

At low conversion, the frequency effect on the viscoelastic behavior is smaller than

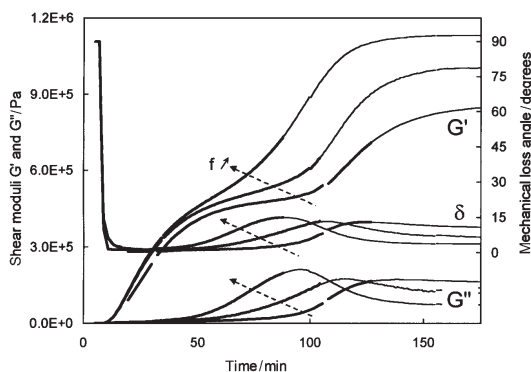


Fig. 10 Influence of frequency: storage and loss shear moduli and mechanical loss angle for the isothermal cure of an unsaturated polyester at 50°C for frequencies (f) of 1, 0.1 and 1/60 Hz. Moduli on linear scale to enlarge the effect of vitrification

at high conversion. For higher conversions, with increasing frequency the viscoelastic behavior is shifted towards the energy elastic state and vitrification is shifted to lower reaction times (Fig. 10). For a 1/60 Hz frequency, the mechanical loss angle δ decreases only slightly after the maximum, more closely resembling the heat flow phase behavior observed in TMDSC at the same frequency (Fig. 3). For the same frequency (1/60 Hz), the onset of vitrification is earlier in TMDSC than in the corresponding dynamic

rheometry experiment (Table 2). However, when comparing these two techniques the following remarks should be made:

(i) Due to the larger sample mass and the less accurate temperature control of the rheometer, small deviations in the temperature profiles exist.

(ii) The reaction in the rheometer occurs in non-hermetic conditions. At the outer circumference of the sample styrene can evaporate, changing the chemical composition.

(iii) Even at the same frequency, differences in glass transition temperatures and in onset of vitrification can be expected because the techniques solicit the material in a different way. Similar differences are noted between glass transitions obtained by TMDSC and DEA (e.g. [42]).

For the final evolution, at lower frequencies (i) G' increases later and reaches a lower final level, (ii) the maximum in G'' (and δ) shifts to higher reaction times, and (iii) δ (and G'') remain at a higher final level. The qualitative evolution of the final levels are supported by dynamic mechanical analyses of fully cured samples: the storage moduli and mechanical loss angles measured at 50°C were 320 MPa and 27° (1 Hz), 88 MPa and 35° (0.1 Hz), and 75 MPa and 44° (1/60 Hz).

Conclusions

The combined use of TMDSC and dynamic rheometry is very beneficial for an isothermal study of gelation, vitrification and autoacceleration (gel effect) in terms of reaction conversion of an unsaturated polyester resin. Comparison of dynamic rheometry and TMDSC results indicates gelation occurs closely after the onset of the reaction exotherm, at a conversion lower than 5%. The onset of vitrification observed in TMDSC by the start of the final decrease in heat capacity and in dynamic rheometry by the final increase in G' occurs at a conversion close to 80%.

An important autoacceleration occurs in between both transitions, the maximum cure rate being closely before the onset of vitrification. The conversion at the heat flow minimum, which can be considered as a measure of the onset of autoacceleration, is close to 60%. Thus, the term gel effect for indicating the autoacceleration is somewhat misleading and should be avoided in this case. The fact that autoacceleration occurs in the later stages of the reaction, whereas gelation happens at the very beginning, indicates the former is not due to the sharp increase in bulk viscosity at gelation, but rather to a change in molecular mobilities at higher conversion. This effect of changing (decreasing) molecular mobilities on the (increasing) reaction rate of the unsaturated polyester system is caused by the specific features of a free radical chain-growth polymerization mechanism and is in contrast with thermosetting systems, such as epoxy-amines, obeying an addition step-growth polymerization mechanism.

* * *

The authors would like to thank Stephane De Backer of TA Instruments Benelux for performing the dynamic mechanical analyses.

References

- 1 G. A. O'Neil and J. M. Torkelson, *TRIP*, 5 (1997) 349.
- 2 G. M. Burnett and H. W. Melville, *Proc. R. Soc. London*, 189 (1947) 494.
- 3 R. G. W. Norrish and E. F. Brookman, *Proc. R. Soc. London. Ser. A*, 171 (1939) 147.
- 4 R. G. W. Norrish and R. R. Smith, *Nature*, 150 (1942) 336.
- 5 E. Trommsdorff, H. Köhle and P. Lagally, *Makromol. Chem.*, 1 (1948) 169.
- 6 G. V. Schulz and C. Harborth, *Makromol. Chem.*, 1 (1947) 106.
- 7 J. N. Cardenas and K. F. O'Driscoll, *J. Polym. Sci., Polym. Chem. Ed.*, 14 (1976) 883.
- 8 B. O'Shaughnessy and J. Yu, *Macromolecules*, 27 (1994) 5067; *Macromolecules*, 27 (1994) 5079.
- 9 A. Faldi, M. Tirell and T. P. Lodge, *Macromolecules*, 27 (1994) 4176.
- 10 M. B. Wisnudel and J. M. Torkelson, *J. Polym. Sci., Polym. Phys. Ed.*, 34 (1996) 2999.
- 11 P. J. Halley and M. E. Mackay, *Polym. Eng. Sci.*, 36 (1996) 593.
- 12 A. Y. Malkin and S. G. Kulichikhin, *Adv. Polym. Sci.*, 101 (1992) 217.
- 13 H. H. Winter, 'Gel point' in 'Supplement to Encyclopedia of polymer science and engineering', 2nd ed., John Wiley, New York 1988, p. 343.
- 14 H. H. Winter, *Polym. Eng. Sci.*, 27 (1987) 1698.
- 15 K. te Nijenhuis, *Adv. Polym. Sci.*, 130 (1997) 1.
- 16 C. Y. M. Tung and P. J. J. Dynes, *J. Appl. Polym. Sci.*, 27 (1982) 569.
- 17 T. Imai, *J. Appl. Polym. Sci.*, 11 (1967) 575.
- 18 J. H. L. Henson, A. J. Lovett and G. S. Learmonth, *J. Appl. Polym. Sci.*, 11 (1967) 2543.
- 19 M. R. Kamal, S. Sourour and M. Ryan, *Soc. Plast. Eng., Tech. Pap.*, 19 (1973) 187.
- 20 M. R. Kamal and S. Sourour, *Polym. Eng. Sci.*, 13 (1973) 59.
- 21 C. D. Han and K.-W. Lem, *J. Appl. Polym. Sci.*, 28 (1983) 3155.
- 22 C. D. Han and K.-W. Lem, *J. Appl. Polym. Sci.*, 29 (1984) 1879.
- 23 D. S. Lee and C. D. Han, *J. Appl. Polym. Sci.*, 34 (1987) 1235.
- 24 K. de la Caba, P. Guerrero, A. Eceiza and I. Mondragon, *Polymer*, 37 (1996) 275.
- 25 C. P. Hsu and L. J. Lee, *Polymer*, 32 (1991) 2263.
- 26 C. P. Hsu and L. J. Lee, *Polymer*, 34 (1993) 4516.
- 27 Y. S. Yang and L. J. Lee, *Polym. Proc. Eng.*, 5 (1987) 327.
- 28 K. S. Anseth, C. M. Wang and C. N. Bowman, *Macromolecules*, 27 (1994) 650.
- 29 C. Y. Yap and H. L. Williams, *Polym. Eng. Sci.*, 22 (1982) 254.
- 30 J. K. Gillham and J. B. Enns, *TRIP*, 2 (1994) 406.
- 31 J. F. Stevenson, *Polym. Eng. Sci.*, 26 (1986) 746.
- 32 G. L. Batch and C. W. Macosko, *J. Appl. Polym. Sci.*, 44 (1992) 1711.
- 33 J. L. Martin, A. Cadenato and J. M. Salla, *Thermochim. Acta*, 306 (1997) 115.
- 34 G. Van Assche, A. Van Hemelrijck, H. Rahier and B. Van Mele, *Thermochim. Acta*, 268 (1995) 121.
- 35 G. Van Assche, A. Van Hemelrijck, H. Rahier and B. Van Mele, *Thermochim. Acta*, 286 (1996) 209.
- 36 G. Van Assche, A. Van Hemelrijck, H. Rahier and B. Van Mele, *Thermochim. Acta*, 304–305 (1997) 317.
- 37 S. Swier, G. Van Assche, A. Van Hemelrijck, H. Rahier, E. Verdonck and B. Van Mele, *J. Therm. Anal. Cal.*, 54 (1998) 585.
- 38 G. Van Assche, A. Van Hemelrijck and B. Van Mele, *J. Thermal Anal.*, 49 (1997) 443.
- 39 S. Montserrat and I. Cima, *Thermochim. Acta*, 330 (1999) 189.
- 40 A. Van Hemelrijck, PhD Thesis, Vrije Universiteit Brussel, Brussel 1996.
- 41 C. P. Hsu and L. J. Lee, *Polymer*, 34 (1993) 4496.
- 42 A. Hensel, J. Dobbertin, J. E. K. Schawe, A. Boller and C. Schick, *J. Thermal Anal.*, 46 (1996) 935.